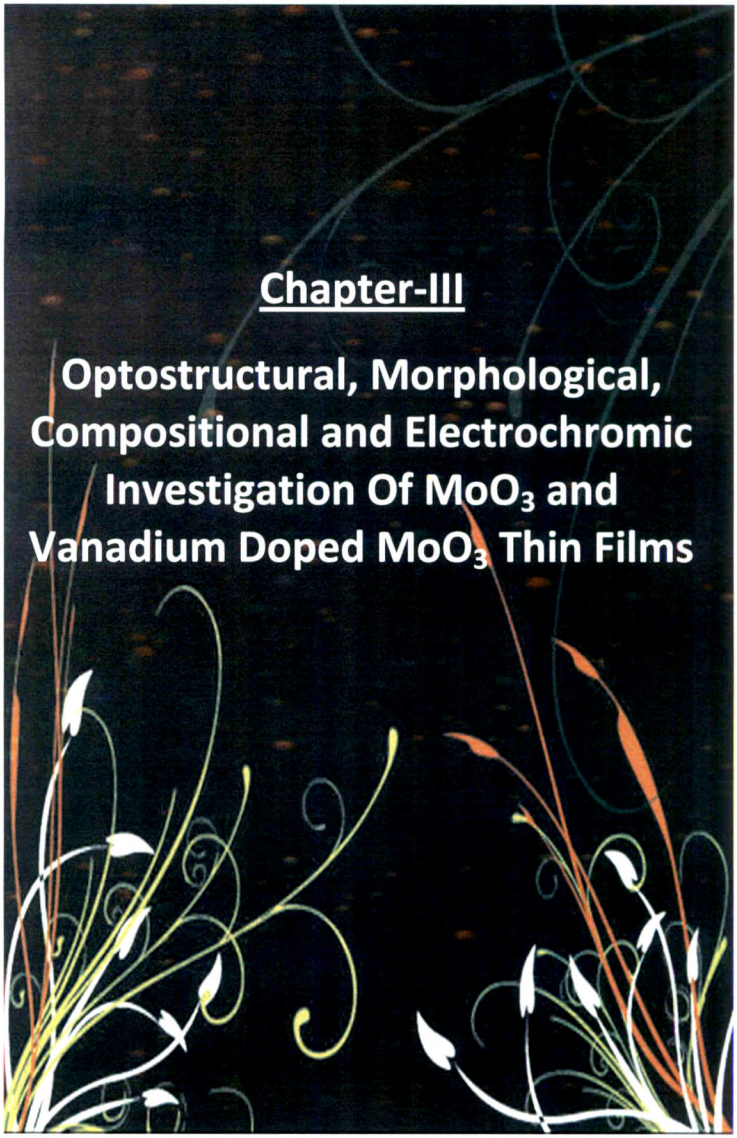

Chapter-III

Optostructural, Morphological, Compositional and Electrochromic Investigation Of MoO_3 and Vanadium Doped MoO_3 Thin Films

CHAPTER III

OPTOSTRUCTURAL, MORPHOLOGICAL, COMPOSITIONAL AND ELECTROCHROMIC INVESTIGATION OF MoO_3 AND VANADIUM DOPED MoO_3 THIN FILMS

CHAPTER III

OPTOSTRUCTURAL, MORPHOLOGICAL, COMPOSITIONAL AND ELECTROCHROMIC INVESTIGATION OF MoO_3 AND VANADIUM DOPED MoO_3 THIN FILMS

Introduction

A brief idea of various techniques of the thin film preparation are outlined in chapter I. Chapter I gives detailed account of the experimental procedure and technical knowledge how that are generated in synthesizing molybdenum oxide and vanadium doped molybdenum oxide thin films.

Many experimental methods, originally designed to study the chemical & physical behavior of solids & liquids have grown into a new field known as materials characterization. During the last 30 years a most techniques aimed to study the surface properties & thin films have been added to the many tools for the analysis of bulk samples. The film has benefited particularly for the development of computers & microprocessors, which have vastly increased the speed and accuracy of measuring devices & the recording of their output materials. Characterization is a very important tool for searching new physical & chemical phenomenon. As it plays essential role in new application of solids in science & technology.

This chapter deals with the optostructural, morphological, compositional and electrochromic studies on chemically synthesized Molybdenum oxide and Vanadium doped molybdenum oxide thin films. These films are characterised by using UV-Vis-NIR absorption spectroscopy, XRD,SEM,Energy Dispersive Spectroscopy(EDS) and Electrochromic analysis to investigate the optostructural, morphological, compositional and electrochromic studies.

3.1 Chemosynthesis of molybdenum oxide thin films

For the deposition of MoO_3 on glass as well as FTO substrates about 70 ml of the bath solution is prepared by using following procedure. 1.5 g of sodium molybdate was weighed and placed in a 100ml beaker . The salt was dissolved in 70 ml distilled water. In the prepared solution of sodium molybdate, 3ml slightly acidic diehtyl sulphate was added. After stirring the

main volume of the sulphate remains insoluble as a second phase. The glass substrates are immersed and the solution is heated on the plate of a magnetic stirrer. With the progressive increase in temperature to a maximum of 95°C, the molybdenum oxide starts to deposit on the glass substrates after a couple of minutes. The deposition time, is 15 min. The maximum thickness of the films from one bath was about 900 nm.

3.2 Chemosynthesis of vanadium doped molybdenum oxide thin film

For the deposition of Vanadium doped MoO_3 on substrates about 70 ml of the bath solution. 1.5 g of sodium molybdate was weighed and placed in a 100ml beaker . The salt was dissolved in 70 ml distilled water. In the prepared solution of sodium molybdate, 3ml slightly acidic diehtyl sulphate was added. After stirring the main volume of the sulphate remains insoluble as a second phase, then 1% of ammonium meta vanadate is added in this order to make the series of vanadium doped molybdenum oxide bath solution for film deposition. The glass substrates are immersed and the solution is heated on the plate of a magnetic stirrer. With the progressive increase in temperature to a maximum of 95°C, the molybdenum oxide starts to deposit on the glass substrates after a couple of minutes. The deposition time, is 15 min. The maximum thickness of the films from one bath was about 900 nm.

3.3 Effect of preparative parameters

The chemical bath deposition technique i.e. solution growth process is now proved to be most suited method for deposition of metal oxide thin films. However growth of the metal oxide film is found to be influenced by the various preparative parameters such as geometry of the substrate holder, speed of substrate rotation ,bath composition , the P^H, deposition time and deposition temperature.

3.3.1 Geometry of the substrate holder

A specially designed substrate holder as shown in figure 3.2 was used for holding the substrate in vertical position. The holder was fabricated by using bakelite material of appropriate thickness. It is a circular disc slotted to fix the substrate in such a fashion that each of the substrate was exactly

perpendicular to each other. The continuous proper bulk churning of the solution in the reaction container was made possible which help in depositing uniform and better orientation of the crystallites. In order to rotate the substrate in a reaction container the substrate holder is attached to rotating shaft of constant speed, A. C. gear Remi make electric motor.

3.3.2. Speed of substrate rotation

The deposition of the metal oxide thin film on the substrate material is greatly influenced by the speed of substrate rotation , at lower speed (say below 40 rpm) thick , porous and non –adherent films were obtained at higher speeds (say above 70rpm) very thin adherent and reflecting film deposition was obtained. Hence in the present investigation the speed of the substrate rotation was kept at optimum value of 50 rpm so as to obtain uniform and adherent metal oxide films on the substrate surface.

3.3.3. Bath composition

The growth rate and quality of the deposited films was greatly influenced by the concentration of the reacting species. Therefore we have studied the effect of concentration of reacting species for various concentrations. The film deposited by using low concentration was thin and non- uniform. This observation a be related to the insufficient supply of ionic species at such concentration level. On the other hand when concentration of species was increased, the quality and uniformity of the films goes on increasing and films were thick. This is true up to a certain level of concentration and then saturation in the growth process was observed.

3.3.4 pH

The simple chemical bath deposition process used for growth of oxide thin films largely depends on pH value of reacting solution. The oxides are well known to be pH sensitive. Increase in the pH value causes increase in the relative molecular surface area and solubility. At slightly acidic pH uniform crystallite site and uniform thin film observed

3.3.5. Deposition time

The growth rate was also studied for various deposition durations. Growth of the thin film is time dependent; hence the deposition of the film was varied from 5 to 20 min depending upon the thickness of film. The deposition of time of 20 min was therefore kept constant throughout.

3.3.6 Deposition temperature

The temperature dependence of growth rate shown by literature survey that the rate of deposition increases with bath temperature resulting in to formation of fine grained structure. But optimum temperature selected for the deposition is 90 to 95 °C.

3.4 Optostructural, morphological, compositional, investigation of MoO_3 thin films

3.4.1 Optical absorption

This is an important technique to know the type of transitions, absorption coefficient& the energy gap (Eg) of the thin film material under study. The optical absorbance of the thin film measured as a function of the wavelength. For optical absorbance measurement HITACHI model 330 JAPAN make UV-visible spectrophotometer was used.

The value of band gap is then determined by plotting the graph of $(\alpha h\upsilon)^2$ vs. $h\upsilon$ The optical absorption spectra of various thin films corrected for glass substrate absorption were obtained in the wavelength range from 350 to 600 nm.The results from these spectrums were analyzed to evaluate the absorption coefficient (α), optical gap (Eg) and the nature of transitions involved.

The plots of $(\alpha h\upsilon)^2$ vs. $h\upsilon$ are linear in the high energy region indicating direct type of transitions in these films. MoO_3 thin film shows direct band gap of 3.1 eV and Vanadium doped MoO_3 thin film shows direct band gap 2.8 eV respectively.

It shows that doping level decreases direct band gap.The nature of graph reveals that optical absorption in these samples takes place through direct band transition.

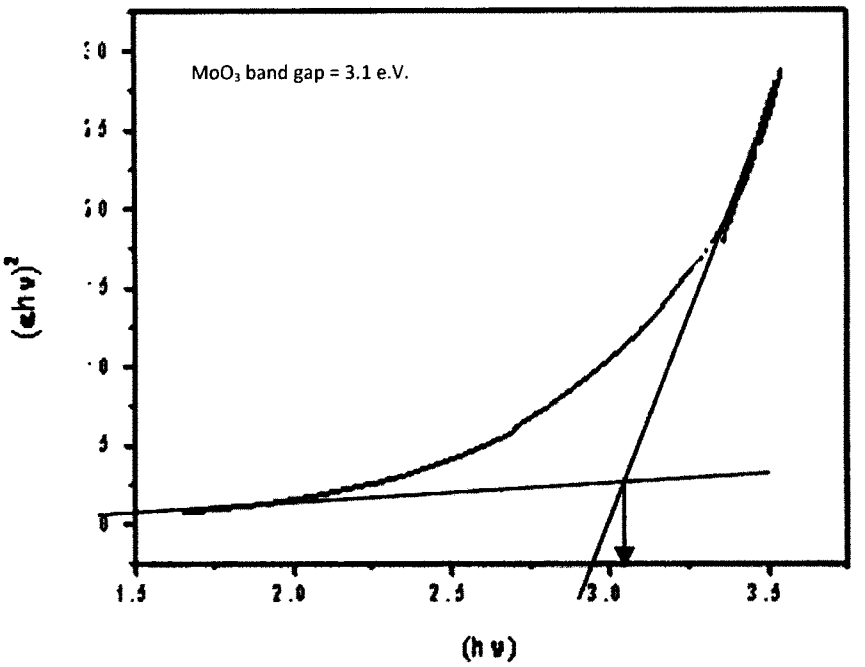

Fig.3.4.a. The plot of $(\alpha h\nu)^2$ Vs $h\nu$ of MoO_3 thin film

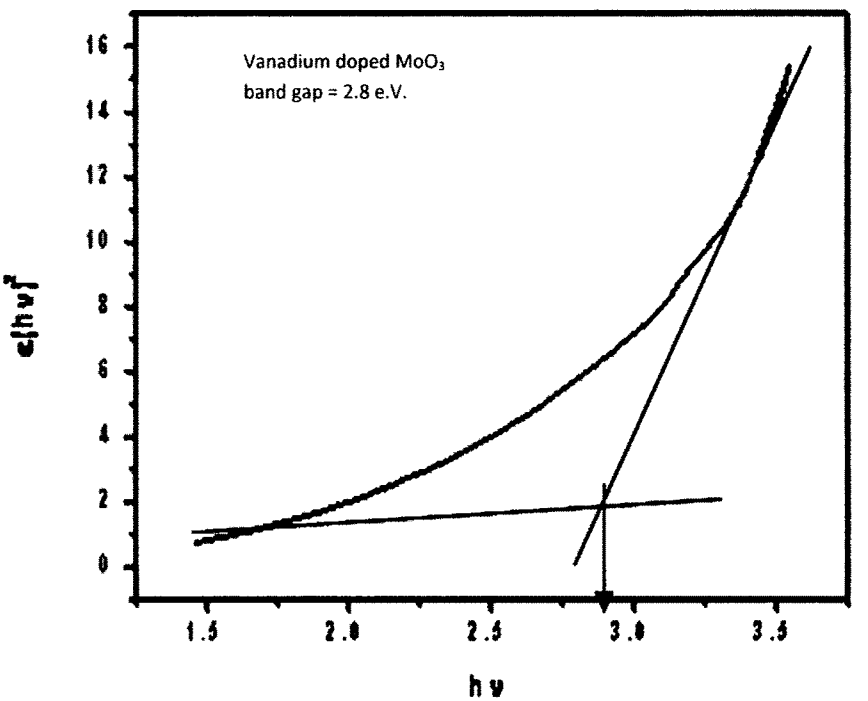

Fig.3.4.b. The plot of $(\alpha h\nu)^2$ Vs $h\nu$ of Vanadium doped MoO_3 thin film

3.4.2. X ray diffraction studies

If the substance is crystalline, identification is usually carried out by X-ray diffraction. Each crystalline solid has its own characteristics X-ray powder pattern which may be used as a 'fingerprint' for its identification. The powder

patterns of most known inorganic solids are includes in an updated version of the Powder Diffraction File; by using an appropriate search procedure, unknowns can usually identified rapidly and unambiguously. Once the substance has been identified, the next stage is to determine its structure and its crystallite size.

An X-ray powder diffraction pattern is a set of lines or peakes, each of different intensity and position (d-spacing or Bragg angle, θ), on either a strip of photographic film or on a chart paper. For a given substance the line positions are essentially fixed and are characteristics of that substance. The intensities may vary somewhat from sample to sample, depending on the method of preparation and the instrumental conditions. For identification purposes, principle note is taken of line positions together with a semiquantitative consideration of intensities. X-ray powder diffraction may be used to measure the average crystallite size in a powdered sample, provided the average diameter is less than about $2000A^0$. The broadening of lines increases with decreasing particle size. The limit is reached with particle diameters in the range roughly 20 to 100 A^0.

In our study, X- ray diffraction (XRD) analysis was carried out using a Philips PW-1710 X-ray diffractometer for the 2θ ranging from 0^0 to 100^0 with Cu K_α line used as a beam (λ=1.5418A^0).

XRD of as deposited MoO_3 and Vanadium doped MoO_3 films show an amorphous nature as no diffraction peak is seen in the respective diffractograms.(fig 3.4.2.a, b, c and d). Figure 3.4.2.a,b,c and d shows XRD patterns of MoO_3 films that were formed at heat treated temperature 500^0C in the air. The heat treatment process changes the film's structure from amorphous to crystalline. The MoO_3 films treated below 300^0c were completely amorphous, without yielding any significant diffraction peaks.Morever,the onset of the crystallization appears at a temperature of 500^0C.

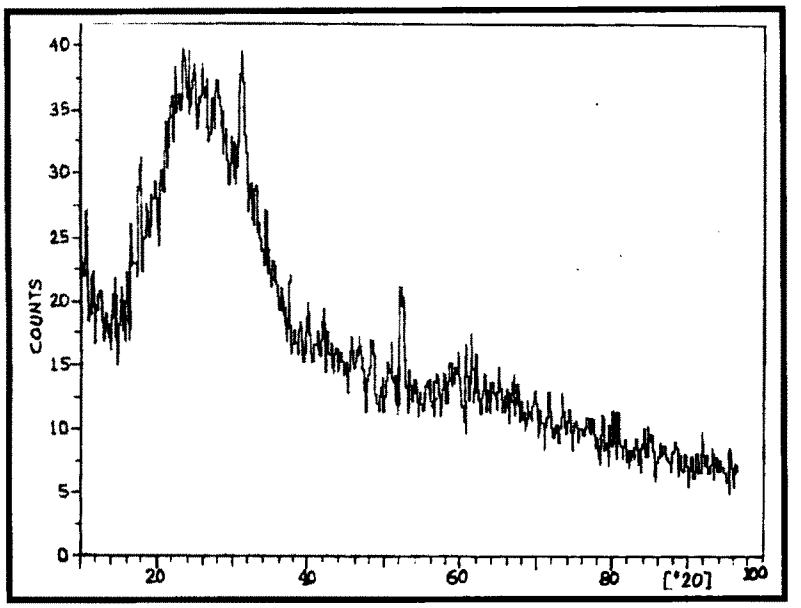

Fig.3.4.2.a. XRD of as deposited MoO_3 thin film

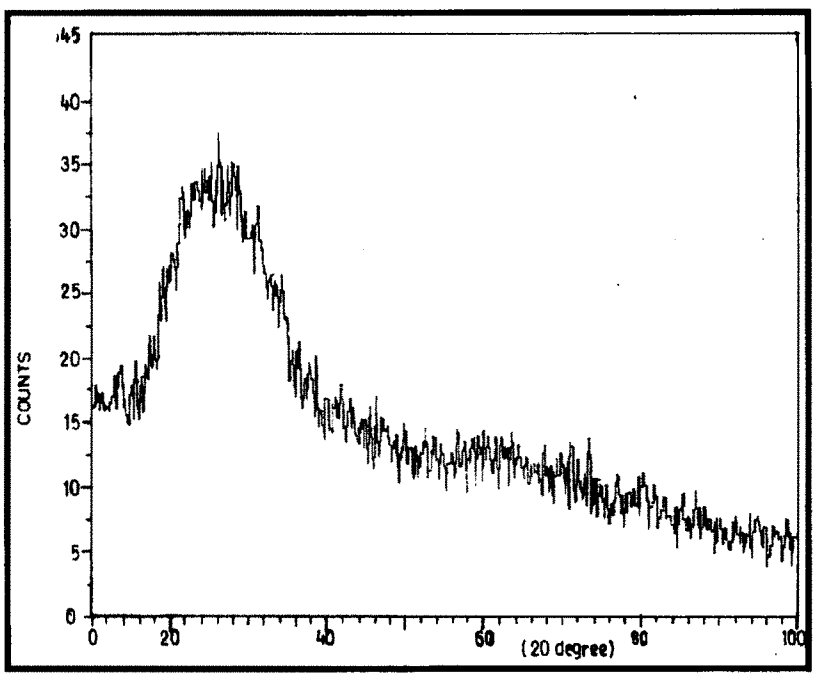

Fig.3.4.2.b. XRD of as deposited Vanadium doped MoO_3.

High intensity peaks in diffractograms of films annealed at 500°C reveal the completeness of crystallization process.

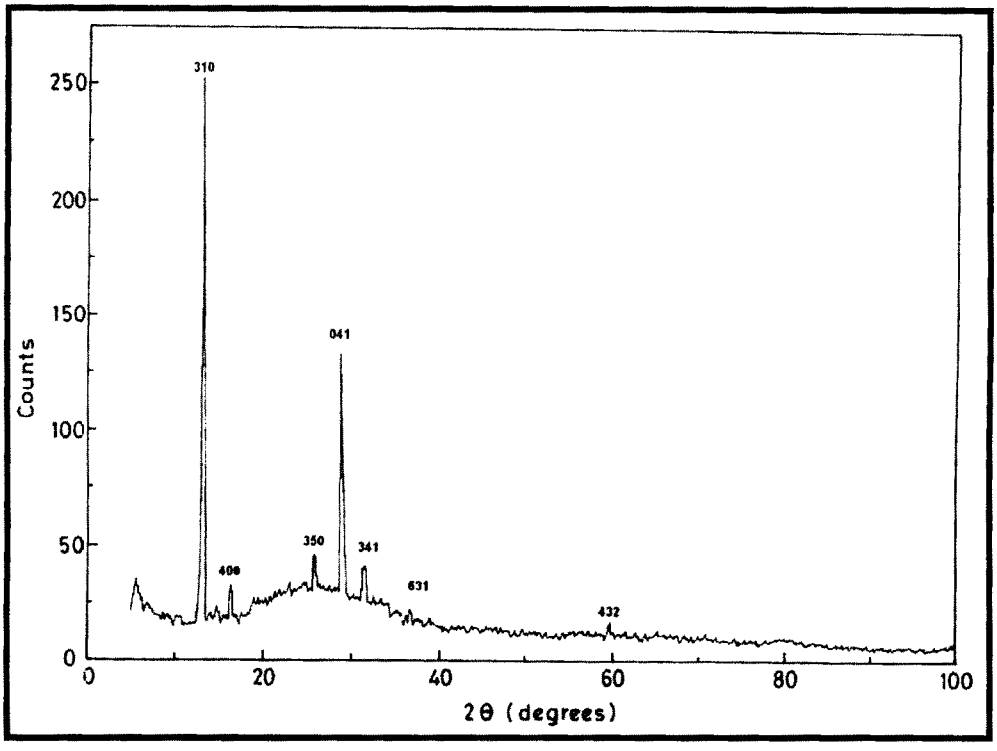

Fig.3.4.2.c XRD of MoO_3 thin film annealed at 500°C.

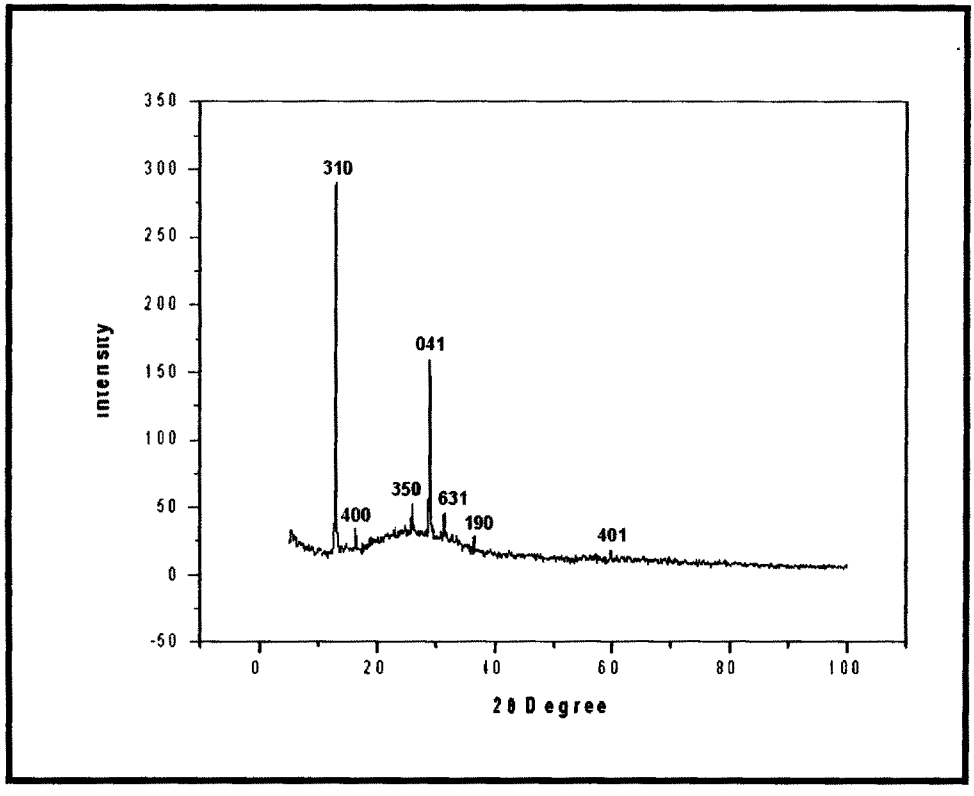

Fig.3.4.2.d.XRD of Vanadium doped MoO_3 at 500°C

The analysis of x-ray diffraction pattern shows the formation of polycrystalline Orthorhombic α-MoO_3 .The d values of observed reflections were compared with the standard d values from JCPDS cards (72-0448 and 71-0566). The d values along with Miller indices (hkl) planes are as shown in table No.3.4.1 and 3.4.2. The lattice constant evaluated for orthorhombic α-MoO_3 unit cell are a=24.49, b=5.457and c=6.752 for card (72-0448) and a=21.531(4), b=19.534(4) and c=4.001.

Table No. 3.4.1. hkl plane and 'd' values of MoO_3 thin film.

Sr. No.	hkl Planes	d cal (A°)	d obs (A°)
1	(310)	6.7366	6.8253
2	(311)	3.7656	3.7937
3	(350)	3.4313	3.4695
4	(701)	3.1063	3.1016
5	(341)	2.8419	2.8351

Table No. 3.4.2. hkl plane and 'd' values of Vanadium doped MoO_3 thin film.

Sr.No.	hkl planes	d cal (A°)	d obs (A°)
1	(310)	6.5802	6.5702
2	(140)	4.7240	4.7325
3	(110)	3.5543	3.5542
4	(401)	3.0983	3.0988

These values are in good agreement with literature data.

It was seen that, the crystallization process begins with the formation of mixed β and α phases. A polymorphic transition from monoclinic-β-phase to orthorhombic α-phase is seen beyond 400 °C.Morever, the (310) crystalline peaks become more strong after the film has been treated at 500^0C. The full-width at haif maximum (FWHM) of (310) peak is narrow shows that the film was crystallized in large grains.Therefore,the

crystallization process strongly depends on the treated temperature.In contrast with the pure MoO_3 film, there is a little shift of the peak toward lower diffraction angle with Vanadium doping,which is corresponding to the increase of the interlayer distance from due to the partial replacement of Mo atoms in MoO_3 with a larger ionic radius.In addition, Vanadium oxide peak is not observed in XRD patterns,which is possible related with that vanadium precursor in doped thin films forms some amorphous oxide or solid solution with MoO_3.There are two reasons responsiblr for this.One probable reason is that it cannot br detected by XRD.The other is that the structure of Mo^{6+} and V^{5+} ions are very similar and the vanadium ions maybe insert into structure of MoO_3

The grain size was determined using Debye Scherer's formula. The grain size increases with increases in temperature. The grain size was found to vary from as shown in table no.3.4.3

Table 3.4.3 Crystallite Size of MoO_3 and Vanadium doped MoO_3 thin films at 500^{0}C temperature

Samples	Temperature °C	Crystallite size nm
MoO_3	500	47
V Doped MoO_3	500	57

3.4.3. Scanning electron microscopy

To observe the external morphology and average grain size of the MoO_3 and Vanadium doped MoO_3 thin film material, JEOL- 6360 Energy Dispersive X-ray Analyzer was used. The thin film samples were cut into 1 cm^2 pieces & mounted on the sample holder with conducting paste. The samples were coated with a thin layer of gold in polar on coating unit E5000 to prevent charging of the samples. The micrographs of the samples were recorded with a 20kv EHT & 25 PA cameras attached on the high resolution-recording unit.

The surface morphology of the thin film material was examined through a scanning electron microscopy. From SEM study it is observed that,

less uniformly distribution of particles with large intergrannular spacing in them. The average grain size which is calculated by linear intercept technique formula is 565.94nm for MoO_3 and 560.23 nm for Vanadium doped MoO_3.It was observed that grain size decreases with Vanadium doping.The Vanadium doped MoO_3 film shows that small Vanadium particles were segregated on the surface of the film.It is seen that Vanadium doping can lead to significant surface morphology changes in MoO_3 films.It is also seen that the nano particles are well synthesized, and have a fine and round grain shaped structure.In the case of the Vanadium doping partial agglomeration of particles of particles. The Fig 3.4.3. a and b Shows scanning images of MoO_3 and Vanadium doped MoO_3 thin films.

3.4.3 a. SEM of MoO_3 thin film

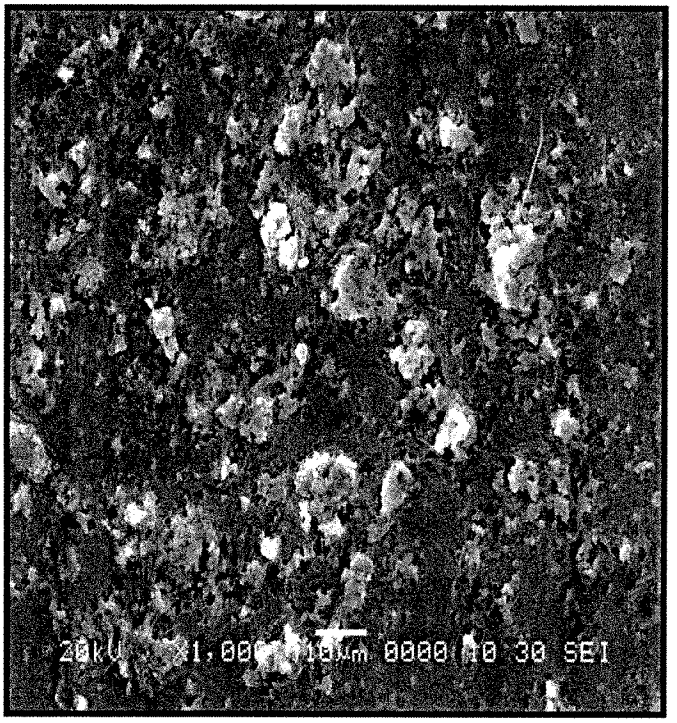

3.4.3 b. SEM of Vanadium doped MoO_3 thin film

3.4.4. Energy dispersive spectroscopy (EDS)

The combinatorial thin films of MoO_3 and Vanadium doped MoO_3 were analysed using EDS technique. The quantitative analysis by EDS was performed for MoO_3 and Vanadium doped MoO_3 thin films in the sample at different points. Energy Dispersive Spectroscopy was performed on a JEOL-JSM- 6360 Scanning microscope. The chemically deposited MoO_3 and Vanadium doped MoO_3 thin film samples were cut into 1 cm^2 pieces and mounted on the sample holder with a thin layer of gold to prevent charging of the samples. EDS spectrum obtained with an accelerating voltage 10 kV, acquisition time of 1 minute on a film within the precision of the energy dispersive spectroscopy, i.e. ± 2%.

In order to confirm of mixed combinatorial phase of MoO_3 and Vanadium doped MoO_3 thin films was determined from EDS profile of the film. Fig.3.4.4 a and 3.4.4 b shows the EDS pattern of MoO_3 and Vanadium doped MoO_3 thin film. The EDS spectrum of MoO_3 shows the presence of Mo and O, in the film. The atomic percentage for Mo and O obtained from the EDS analysis is 12.80 and 87.20 respectively. The EDS spectrum of Vanadium doped MoO_3 shows the presence Mo,O and Vanadium in the film. The atomic percentage for Mo, O and Vanadium obtained from the EDS analysis is 20.31, 74.08 and 5.61 respectively.

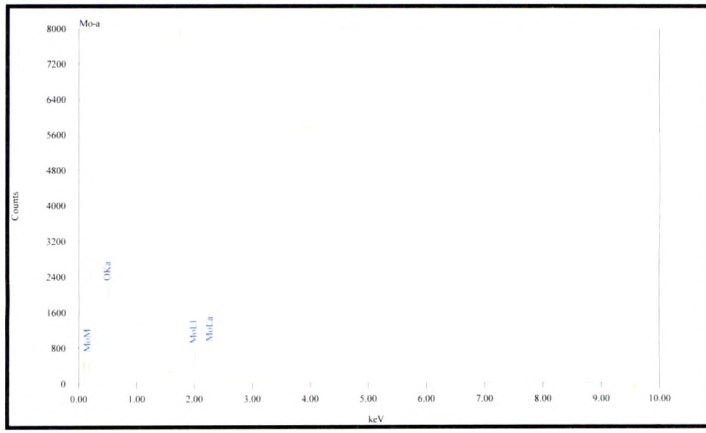

Fig. 3.4.4 a. EDS spectrum of MoO_3 thin film

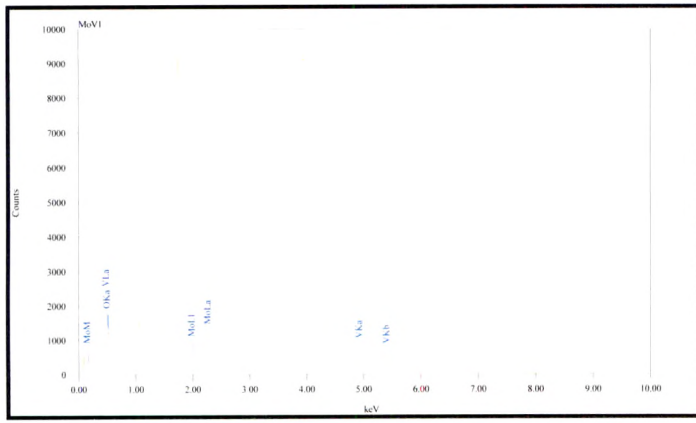

Fig. 3.4.4 b EDS pattern of Vanadium doped MoO_3 thin film

3.5 Electrochromic characterisation

3.5.1 Electrochromic applications of MoO_3 thin films

The first successful demonstration of an electrochromic device with controllable light absorption, transmission, or reflection has raised considerable interest in the fabrication of a number of electro-optic devices (as shown by the issuance of several hundred patents worldwide during the last two decades). The initial excitement on this technology has been somewhat dampened by the realization that the operation of this device depends on ion transport, which necessarily limits the response time to the milliseconds regime. However, this phenomenon can be exploited for a good variety of applications, where very fast response times are not essential. Consequently, much effort is presently being devoted to the fabrication of devices such as "smart windows," with controllable absorption and reflection in the visible and near-infrared region; automobile rearview mirrors, which modulate the reflectance and hence control the glare; high-contrast displays, which offer some advantages over the competing liquid-crystal technology; and a variety of other applications which utilize the unique properties of the electrochromic phenomenon. Extensive work has been done in the past to fabricate display devices that utilize some of the unique properties of this phenomenon, such as high contrast, no angular dependence, continuously variable density of coloration, and memory.

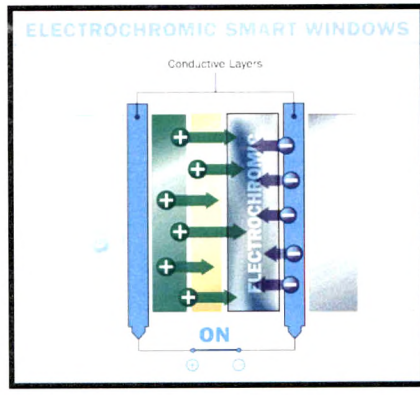

Fig3.5.a. Typical multilayered MoO_3 based electrochromic device for smart windows applications

Most of the display devices are based on a semi-solid structure, in which the electrochromic films are deposited on a suitably patterned transparent electrode, an opaque electrolyte containing H^+ ions or Li^+ ions, and a counter electrode consisting of $HxMoO_3$. Key technological barriers to a successful commercialization of electrochromic displays are the response time and the lifetime. May innovative steps have been taken to address these issues and response times of 50 to 100 ms and lifetimes over 107 cycles have been achieved.

Another very exciting application of a large-area transmissive electrochromic device is in the area of switchable, solar-gain-control building windows, the so-called "smart windows". The automatic control of solar gain through windows offers may advantages, and electrochromic devices are uniquely suited for this. Several different electrochromic materials and device structures are currently Being investigated for this purpose. Asahi Glass of Japan has already developed square-foot-size electrochromic panels and is currently evaluating their performance characteristics. The U.S. Department of Energy is also currently supporting a research and development program in this area. For an electrochromic device to be commercially successful in a window application, it must meet several stringent criteria for performance, durability, aesthetic acceptability, and, above all, cost-effectiveness. At SERI we are currently investigating the fabrication of electrochromic coatings by plasma-enhanced chemical vapor deposition (CVD) which has the potential for significant cost reduction.

One of the success stories of electrochromic devices is the recent introduction of automatic glare control in automotive rear-view mirrors. The basic concept of this device. After years of extensive research, Schott Glass in Germany has fabricated an all-solid-state, reflecting electrochromic mirror which apparently meets the very rigid requirements of an automotive application.

The device takes advantage of variable absorption of the electrochromic layer placed over a metal reflector. Today, electrochromic rearview mirrors are being offered by most of the U.S. manufacturers as a standard feature in some of the more expensive automobiles.

An intriguing application of MoO_3-based electrochromic devices is the fabrication of a solid-state memistor (resistors with memory) for electronic neural networks. The three-terminal transistor-like device uses electrochromic MoO_3 to provide reprogrammable, variable resistance with memory. In this structure, the MoO_3 electrochromic film between the pair of nickel electrodes defines the conducting channel of the memistor. Programming the channel resistanceis accomplished by applying of a voltage to the gate A1 electrode. The resistance of the test structure can be programmed in a reversible manner and can be stabilized at any value in the dynamic range of 10 5 to 10 ° fL Some other potential applications of electrochromic devices include high resolution electrophotographic devices, involving a combination of photoconducting and electrochromic layers that utilize the threshold voltage for coloration; electron beam lithography, which uses differential etching characteristic of the colored and uncolored film; ad photo-electrochemical energy conversion and storage.

In conclusion, the electrochromic phenomenon provides unique opportunities for the fabrication of a multitude of technologically important devices. Since the functionability of the device depends on both electron and ion transport, it is not feasible to achieve a very fast response time. The most successful devices to date use liquid or semi-solid electrolyte as the ion source, and they will ultimately determine the success of this technology; therein lies the greatest challenge. Our basic understanding of the phenomenon itself, with regard to the nature of the color centers and the dynamics of the coloration process, particularly for the solid-state device, is far from complete.

3.5.2 Cyclic voltammetry (CV)

Cyclic voltammograms (CV) were recorded for MoO_3 as well as Vanadium doped MoO_3 films with the linear potential sweep between ± 0.5 V Vs SCE at 10 m/s scan rate and are shown in Figure 3.5.2.a and 3.5.2.b. When a negative potential was applied, a blue colour was observed, indicating oxide reduction followed by H^+ ions intercalation. After the reversal of the potential, the anodic current started to flow, corresponding to the

deintercalation process. There is a well-defined anodic peak for the film, indicating that the H^+ ion insertion–removal process is highly reversible with little hysteresis. The area of the hysteresis curves and the height and position of anodic and cathodic peaks are closely related to the electrochemical processes occurring in MoO_3 and Vanadium doped MoO_3. As we doped vanadium into MoO_3 there is increase in the area of voltammograms and the shift of the threshold voltage (*E_)* towards a positive potential offers an easyway for diffusion and charge transfer process of ions. The cathodic peak current density increases for Vanadium doped films, indicating that the H^+ ions easily diffuse in the mixed phase of Vanadium doped MoO_3 thin films.

In CV potential is swept between two vertex potentials and the current resulting from ion intercalation and deintercalation is measured. In the forward scan rate the current remains close to zero to a certain voltage and then progressively increases and attain maximum. To negative value (cathodic peak current) this corresponds to intercalation (coloring) where the electrons from FTO and H^+ ions from electrolyte are inserted into the MoO_3 and Vanadium doped MoO_3 thin film. During the reverse scan the de-intercalation starts the current passes through a maximum (anodic peak current) and finally becomes zero at certain voltage. The resulting EC coloring/bleaching mechanism is explained in terms of reversible reduction /oxidation between Mo^{+6} and Mo^{+5} ions by Polaron hopping. The film turns blue at - 0.5 vs SCE and it retrieves to it's semitransparent state at it's + 0.5 vs SCE. The intercalation and deintercalation process takes place according to equation 1.1 and 1.2. It was also seen that cathodic peak current (Ipc) and anodic peak current (Ipa) increases in scan rate. (V)

◆ **Diffusion coefficient (D)**

The diffusion coefficient *(D)* of H+ ions during intercalation and deintercalation is calculated by using the Randles–Servcik equation,

$$D^{1/2}=Ip/2.69\times10^5.n^{2/3}.C.A.V^{1/2} \qquad \text{----3.5.1}$$

where ,

Ip=cathodic or anodic peak current

C=Concentration of ionic species

n=ionic charge

A=Area of film

V=Potential Scan Rate

By substituting all the values, the diffusion coefficientat the ±0.5 Vs scan rate is calculated for intercalation and deintercalation processes for the MoO_3 and Vanadium doped MoO_3 thin films

It is the measure of ease with which the ions can intercalate /de intercalated through the host lattice. A linear relationship implies that the reaction is diffusion controlled . The diffusion Coefficient for samples was calculated at different scan rated in the potential window of ±0.5v/s SCE found to be 1.21 X 10^{-10} cm^2/s and 2.64X 10^{-10} cm^2/s for MoO_3 and Vanadium doped MoO_3 thin films for intercalation and de-intercalation respectively.

The observed effect might be due to change in microstructure of MoO_3 with Vanadium doping. Doping improves kinetics of intercalation and deintercalation mechanism charges.

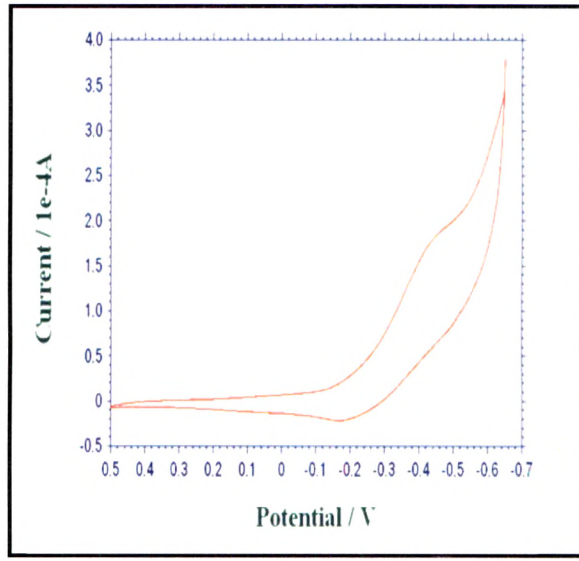

Fig. 3.5.2.a. CV of MoO_3 thin film

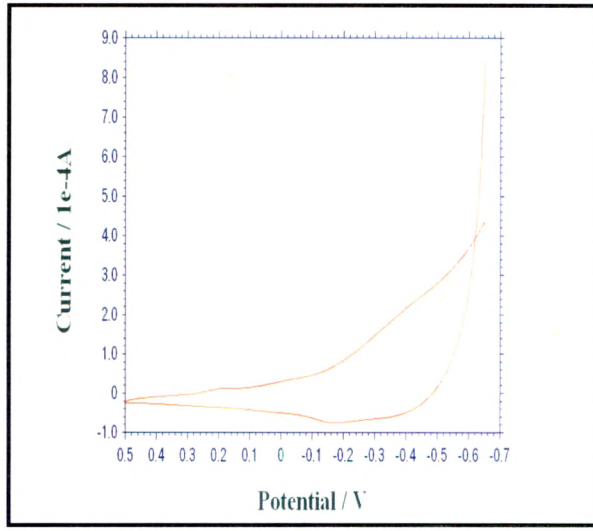

Fig. 3.5.2.b. CV of Vanadium doped MoO_3 thin film

3.5.3 Chronoamperometery (CA)

Chronoamperometry (CA) data were recorded for the MoO_3 and Vanadium doped MoO_3 thin films with the potential being stepped from ±0.5V for 10 s and shown in figure 3.5.3.a. and 3.5.3.b. The higher bleaching current arises from the good conductivity of MoO_3 and Vanadium doped MoO_3 thin films.The higher bleaching current arises from the good conductivity of molybdenum bronze(H_xMoO_3) and rapid decays in current are due to conductor to insulator transition.On the other hand, insulator to conductor transition during coloration is slow. The response times for colouration (*tc)* and bleaching (*t*b*)* were calculated from the CA data from figure 3.5.3.a. and 3.5.4.b. and are listed in table 3.5.1. All the films show fast colour–bleach kinetics.The bleaching kinetics is always faster than the colouring rate owing to the well-defined different mechanisms. The bleaching speed is governed by the space charge limited current flow of cations through the bulk of the film whereas in the colouring mode the potential barrier at the MoO_3 electrolyte interface and the number of H^+ insertion play a critical role.

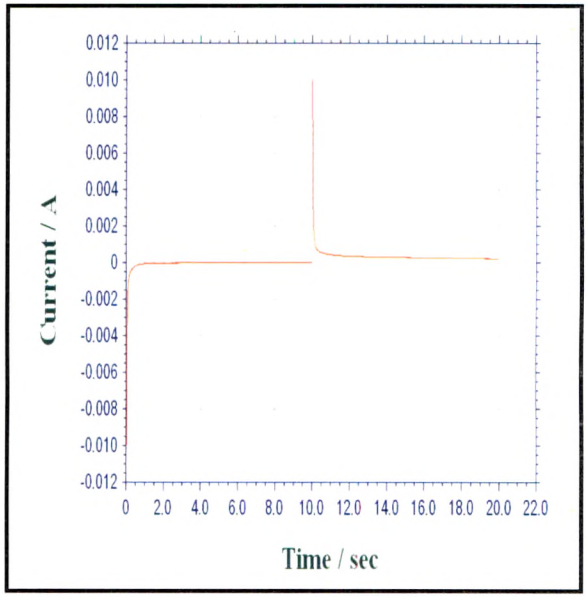

Fig. 3.5.3.a. CA of MoO_3 thin film

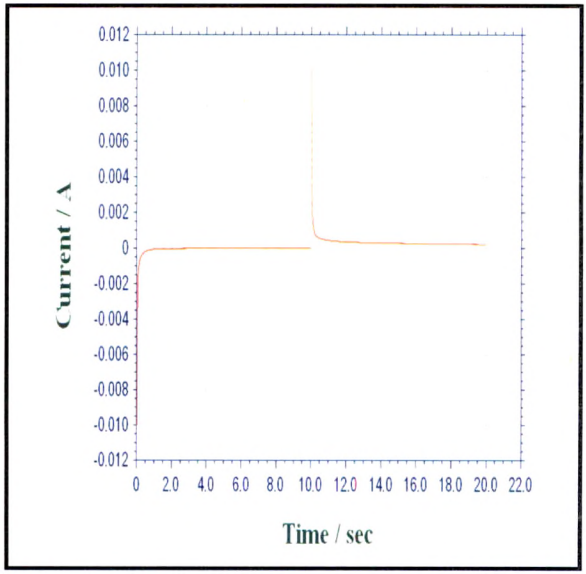

Fig. 3.5.3.b. CA of Vanadium doped MoO_3 thin film

Table No.3.5.1 Response time for MoO_3 and Vanadium doped MoO_3

Samples	Response Time	
	tc(coloring)sec	tb(bleaching)sec
MoO_3	7	4
V doped MoO_3	5	1

3.5.4 Chronocoulometery

The number of H^+ ions intercalated and deintercalated with respect to time was measured using chronocoulometry(CC) studies. Figure 3.5.4.a and 3.5.4.b shows charges intercalated/ deintercalated versus time transients at ±0.5V for the step of 10 s for the MoO_3 and Vanadium doped MoO_3 thin films. In the forward scan the charges are intercalated into the film by a diffusion process resulting in colouration due to reduction of Mo+6 to Mo+5 states. In the reverse scan the intercalated charge is removed from the film, resulting in bleaching due to oxidation of Mo+5 to Mo+6 states. The reversibility of the films was calculated as a ratio of charge de-intercalated (Qdi) to charge intercalated (Qi) in the film.

Quantitative information about the intercalation/deintercalation mechanism can be obtained by converting current time response .This is called CC, which is integral analogue of chronoamperometery A CC curves gives information about the quantities of intercalated and deintercalated charges which can further used to estimate reversibility. Typical double potential step CC curves for MoO_3 and V doped MoO_3 thin film in the different potential windows are as shown in fig. 3.5.4.a. and 3.5.4.b. It was observed that at the low potential window, the amount of deintercalated charge is greater than the intercalated charge. This is attributed to the presence of adsorbed/absorbed H^+ species. At higher potential window the deintercalated charge is less than the intercalated charge. This can be ascribed to the trapping of H^+ ions into the deeper layers of the sample. At the potential window ± 0.5 V a fairly reversible process was observed .Thus the observed

trend indicating the shallow and deeper penetration at the higher potential window.

The CC curves for the MoO_3 and Vanadium doped MoO_3 are depicted in fig.3.5.4 a and 3.5.4 b. From the observed value of intercalated charge Qi and deintercalated charge Qdi, the reversibility was estimated using equation

$$\text{Reversibility} = Qdi / Qi \qquad \text{---3.5.2}$$

Where,

Qi is amount of charges intercalated

Qdi is deintercalated.

The reversibility was estimated for MoO_3 is 55% and for Vanadium doped MoO_3 is 73% respectively. Reversibility increases with doping.The observed improvement in the reversibility may be attributed to the change in microstructure of MoO_3 thin films on Vanadium doping, in comparision with pure MoO_3 thin films.The effect of Vanadium doping in MoO_3 is two fold,one in terms of adsorption of water molecules as both Vanadium and MoO_3 are hydrophilic.Such physisorbed water content gives marginal enhancement to the ion intercalation/deintercalation process,consequently leading to increase in electrochromic reversibility.Secondly Vanadium restricts the extent of crystallization of MoO_3 thin films, thereby retaing amorphisity of MoO_3 which is favourable for easy intercalation and deintercalation of the ions. Chronocoulometry estimated that reversibility increase with Vanadim doping in MoO_3 thin films.

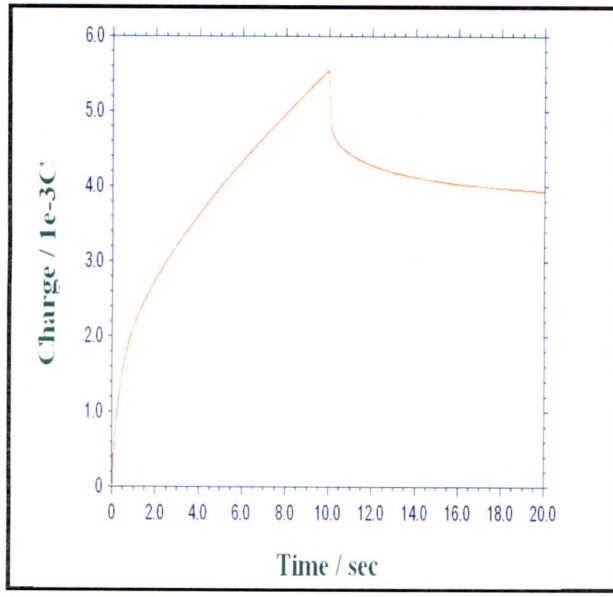

Fig. 3.5.4.a. CC of MoO_3 thin Film

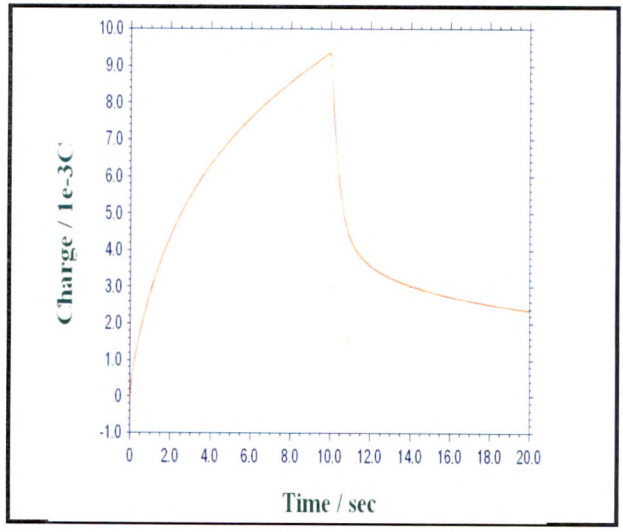

Fig. 3.5.4.b. CC of Vanadium doped of MoO_3 thin Film

3.6 Conclusions

Chemical bath deposition technique is applied successfully for the synthesis of stichiometric, adherent and uniform thin films of transition metal oxides. Optical absorption studied of transition metal oxide shows that band gap decreases with Vanadium doping.X-ray diffraction confirmed the different phase formation on doping of Vanadium in MoO_3 thin films. The films are mechanically stable no cracksand voids are observed in the low magnification SEM image. The electrochromic studies shows that Vanadium doping in MoO3 thin films enhances electrochromism.The Cyclic voltametery studied shows that Vanadium doping improves kinetics of intercalation and deintercalation mechanism charges.A linear relationship implies that the reaction is diffusion controlled. Chronoamperometry studies show the response times for coloration and bleaching are faster due to Vanadim doping.

References

1 S.H.Lee, M.J.Seong, C.E.Tracy, A.Mascrarenhas, J.R.Pitts, S.K.Deb, *Solid State.* **147** (2002) 129.

2 K.Gesheva, M.Surtchev, T.Ivanova, *Solar Energy Mater. Solar Cell.* **76** (2003) 563.

3 J.Okumu, F.Koerfer, C.Salinga, M.Wuttig, *J.Appl.Phys.* **95** (2004) 7632.

4 T.S.Sian, G.B.Reddy, *Appl.Surf.Sci.* **236** (2004) 1.

5 S.H.Lee, M.J.Seong, C.E.Tracy, A.Mascrarenhas, J.R.Pitts, S.K.Deb, *Solid State.* **147** (2002) 129.

6 K. Bange, Sol. Energy Mater. Sol. Cells. **58** (1999) 1.

7 B. Forslund, J. Chem. Ed. **74** (1997) 8.

8 R. Reisfeld, Smart Optical Materials by Sol-Gel Method, (2000).

9 Yoshimura T 1985 J. Appl. Phys. **57** 911.

10 T. Nanba, T. Takahashi, J. Takada, A. Osaka, Y. Miura, I. Yasui, A. Kishimoto, T. Kuda, J. Non-Cryst. Solids. **178** (1994) 233.

11 D. Davazoglou, A. Donnadieu, A. Donnadieu, Sol. Energy Mater. **71** (1988) 379.

12 R. Hurdich, Electron. Lett. **11** (1975) 142.

13 K.D. Lee, Thin Solid Films. **302** (1997) 84.

14 P.M.S. Monk, L.S. Chester, Electrochim. Acta. **38** (1993) 1521.

15 Z. Yu, X. Jia, J. Du, J. Zhang, Sol. Energy Mater. Sol. Cells. **64** (2000) 55.

16 B.Orel,U.Opara,U.Lavrenele Stangar,P.Judemstein. J.Sol-Gel Sci. Technol. **11** (1998) 87.

17 S. Castro-Garcia, B. Pecquenard, A. Bender, J. Livage, C. Julien, Ionics. **3** (1997) 104.

18 Inorganic Index to the Powder Diffraction File, Join Committee on The Powder Diffraction Standards (1972).

19 M.Nagasu,N.Koshida. Appl.Phys.Lett. **57** (1990) 1324.

20 M. Green,W.C.Smith,J.A.Welner.Thin Solid Films. **38** (1976) 89.

21 R.S.Mane,C.D.Lokhande,Mater.Chem.Phys. **65** (2000) 1.

22 J.Cheng,D.B.Fan, H.Wang,B.W.Liu,Y.C.Zhang,H.Yan.Semicond. Sci.Technol.**18** (2003) 676.

23 O.Bohnke,C.Bhonke,G.Robert.Solid State Ion. **6** (1982) 121

24 L.H.M.Krings,W.Talen,Sol.Energy Mater.Sol.Cell. **54** (1998) 27.

25 M. Zayat, R. Reisfeld, H. Minti, A. Zastrow. Sol. Energy Mater. Sol. Cell. **54** (1998) 109.

26 Aiping Jin, Wen Chen, Quanyao Zhu, Ying Yang, V.L. Volkov, G.S. Zakharova. Thin solid Films. **517** (2009) 2023.

27 L. Q. Mai, W. Chen, Q. Xu, J. F. Peng, Q. Y. Zhu, Chem. Phys. Lett. **382** (2003) 307.

28 Cholsong Pang, Ji Luo, Zhimeng Guo, Min Guo, Ting Hou. Int. Journal of Refractory Metals & Hard Materials. **28** (2010) 343.

29 R. R. Kharade, S. R. Mane, R. M. Mane, P. S. Patil, P. N. Bhosale. J. Sol-Gel Sci. Technol. **56** (2010) 177.

30 Shih-Yuan Lin, Chih-Ming Wang, Kuo-Sheng Kao, Ying-Chung Chen, Chan-Chih Liu. J. Sol-Gel Sci. Technol. **53** (2010) 51.